Available online at www.sciencedirect.com

ScienceDirect

journal homepage: www.elsevier.com/locate/he

Is steam addition necessary for the landfill gas fueled solid oxide fuel cells?

*Meng Ni**

Building Energy Research Group, Department of Building and Real Estate, The Hong Kong Polytechnic University, Hung Hom, Kowloon, Hong Kong, China

ARTICLE INFO

Article history:
Received 15 August 2013
Received in revised form
29 September 2013
Accepted 1 October 2013
Available online 31 October 2013

Keywords:
Landfill gas
Solid oxide fuel cell
Methane carbon dioxide reforming
Modeling

ABSTRACT

Landfill gas in Hong Kong – a mixture of about 50% (by volume) CH_4 and 50% CO_2 – can be utilized for power generation in a solid oxide fuel cell (SOFC). Conventional way of utilizing CH_4 in a SOFC is by adding H_2O to CH_4 to initiate methane steam reforming (MSR) and water gas shift reaction (WGSR). As the methane carbon dioxide reforming (MCDR: $CH_4 + CO_2 \leftrightarrow 2CO + 2H_2$) is feasible in the SOFC anode, it is unknown whether H_2O is needed or not for landfill gas fueled SOFC. In this study, a numerical model is developed to investigate the characteristics of SOFC running on landfill gas. Parametric simulations show that H_2O addition may decrease the performance of short SOFC at typical operating conditions as H_2O dilute the fuel concentration. However, it is interesting to find that H_2O addition is needed at reduced operating temperature, lower operating potential, or in SOFC with longer gas channel, mainly due to less temperature reduction in the downstream and easier oxidation of H_2 than CO. This preliminary study could help identify strategies for converting landfill gas into electrical power in Hong Kong.

1. Introduction

Municipal solid waste (MSW) in Hong Kong is disposed at 3 landfill stations: West New Territories Landfill at Tuen Mun, North East New Territories Landfill at Ta Kwu Ling, and South East New Territories Landfill at Tseung Kwan O [1]. Through biological, chemical and physical processes, huge amount of landfill gas can be generated. As landfill gas in Hong Kong consists of about 50% (by volume) methane, about 50% carbon dioxide, and small amount of other gases such as nitrogen [1], it can be used as an energy source. However, conventional heat engine is used for power generation from landfill gas in Hong Kong, with a relatively low efficiency (typically 30%).

Solid oxide fuel cells (SOFC) are advanced power generation devices that can convert the chemical energy of a fuel to electricity via electrochemical reactions at efficiency considerably higher than conventional heat engines [2]. Typical SOFC consists of Ni-YSZ (yttria-stablized zirconia), YSZ electrolyte, and lanthanum strontium manganate-YSZ (LSM-YSZ) composite cathode. Operating at a high temperature (i.e. 800 °C), SOFC exhibit several advantages over conventional heat engines and low temperature fuel cells (i.e. PEMFC): (1) fast electrochemical reaction rate; (2) low cost catalyst can be used; (3) high quality waste heat can be recovered for combined heat and power cogeneration or multi-generation thus the system efficiency can be improved; and (4) fuel flexibility – high temperature enables internal reforming of hydrocarbon fuels [3]. In the literature, various alternative fuels have been tested in SOFC for power generation, such as hydrogen, methane, and ammonia [4,5]. Methane has been frequently studied as a

* Tel.: +852 2766 4152; fax: +852 2764 5131.
E-mail addresses: bsmengni@polyu.edu.hk, memni@graduate.hku.hk.

0360-3199/$ – see front matter
http://dx.doi.org/10.1016/j.ijhydene.2013.10.006

typical hydrocarbon fuels for SOFC as it is a major component in natural gas and a key component in renewable biogas [6]. When methane is used as fuel in SOFC, it must be reformed either internally or externally to produce hydrogen and carbon monoxide-rich syngas [7], which is subsequently used in the electrochemical reactions for power generation. Methane steam reforming (MSR) is the most frequently adopted method for converting methane into syngas, as steam is cheap and widely available. In addition to MSR, methane carbon dioxide reforming (MCDR) has been proven to be feasible for syngas production. Experimental studies have also demonstrated the feasibility of landfill gas fueled SOFC for power generation [8]. Staniforth and Kendall [8] mixed Cannock landfill gas with oxygen as a fuel for SOFC, since the CO_2 content in Cannock landfill gas is not sufficient (26% by volume) for complete reforming of CH_4 (56% by volume). They achieved good initial performance but observed performance loss over time due to poisoning with hydrogen sulfide. With desulfurization, the performance stability was improved considerably [8]. A 20 kW SOFC unit has been operating for more than 1500 h on landfill gas, producing electricity for 10 households in Vaasa, Finland [9]. Very recently, a modeling study was reported on SOFC running on CH_4/CO_2 mixture [10]. It was found that the performance of SOFC fueled with CH_4/CO_2 mixture was comparable to that of SOFC with MSR. Since the molar ratio of CH_4/CO_2 in landfill gas in Hong Kong is about 1:1, which is perfect for complete reforming of CH_4 by CO_2, one could expect that the pre-treated landfill gas can be used as fuel in SOFC without adding O_2 or H_2O which may dilute the fuel concentration. However, adding H_2O could favor reversible water gas shift reaction (WGSR), which can produce additional H_2 for power generation. Considering these possible reactions in SOFC, it is still unknown whether addition of H_2O is necessary for landfill gas fueled SOFC. To answer this scientific question, a numerical model is developed to examine the effect of H_2O addition on landfill gas fueled SOFC at various operating conditions. To simplify the analysis, it is assumed that the landfill gas is pre-treated (i.e. desulfurization) so that the impurities have been removed before being supplied to SOFC. As part of an ongoing project, this study offers theoretical guidance for subsequent experimental studies.

2. Model development

Fig. 1 shows the working principles and computational domain of landfill gas fueled SOFC with consideration of H_2O addition in the fuel stream. The 2D domain includes the interconnector, fuel and air channels, porous anode, dense electrolyte and porous cathode. Conventional planar SOFC with Ni-YSZ anode, YSZ electrolyte and LSM-YSZ cathode is considered in the present study. In operation, the landfill gas with or without steam addition is supplied to the anode channel while air is supplied to the cathode. In the anode side, the mixture is transported from the fuel channel into the porous anode layer, where the MCDR, MSR, WGSR take place (Eqs. (1)–(3)).

$$CO_2 + CH_4 \leftrightarrow 2CO + 2H_2 \quad (1)$$

$$CH_4 + H_2O \leftrightarrow CO + 3H_2 \quad (2)$$

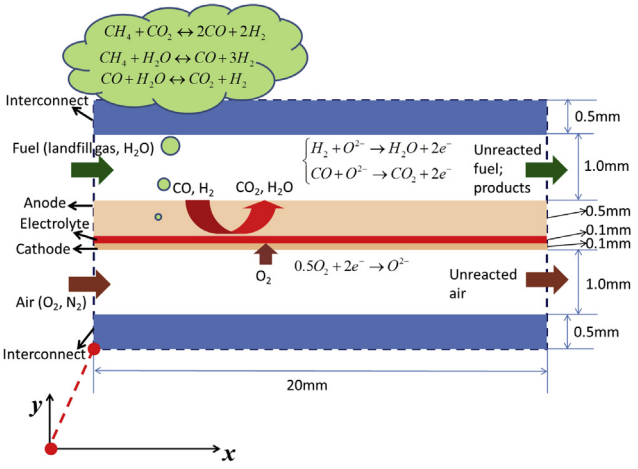

Fig. 1 – Working principles and computational domains.

$$CO + H_2O \leftrightarrow CO_2 + H_2 \quad (3)$$

It should mentioned that even if H_2O is not supplied to the anode channel, the MSR (Eq. (2)) and WGSR (Eq. (3)) can still occur as H_2O can be electrochemically produced in the anode. In addition, the CH_4 decomposition and Boudouard reaction which can cause carbon deposition are not considered [11,12]. With typical SOFC materials (Ni as anode), direction electrochemical oxidation of CH_4 is much slower than that of H_2 and CO and thus is not considered in the present paper. Both H_2 and CO gas molecules diffuse through the porous anode to the triple-phase boundary (TPB) at the anode-electrolyte interface, where they react with oxygen ions to produce electrons, H_2O and CO_2 (Eqs. (4) and (5)).

$$H_2 + O^{2-} \rightarrow H_2O + 2e^- \quad (4)$$

$$CO + O^{2-} \rightarrow CO_2 + 2e^- \quad (5)$$

The electrons produced in Eqs (4) and (5) flow to the cathode side through the external circuit to deliver useful electrical power. At the cathode, oxygen molecules diffuse from the cathode channel to the TPB at the cathode-electrolyte interface, where they react with electrons to produce oxygen ions (Eq. (6)). Subsequently, oxygen ions are conducted to the anode via the dense electrolyte to oxidize H_2 and CO (Eqs (4) and (5)).

$$0.5O_2 + 2e^- \rightarrow O^{2-} \quad (6)$$

Based on the principles, a 2D model is developed to simulate the coupled transport and reaction in landfill gas fueled SOFC.

2.1. *Chemical reactions*

The chemical model is developed to determine the reaction rates and reaction heats of MSR, MCDR, and WGSR. In the present study, it is assumed that all chemical reactions occur in the porous anode layer, neglecting the reaction in the gas channel. The MCDR reaction rate (R_{MCDR}, mol m^{-3} s^{-1}) can be determined with the Langmuir–Hinshelwood (LH) model (for Ru/γ-Al_2O_3/Ni–Cr–Al) as [13],

$$R_{MCDR} = \frac{k_{CO_2} K_{CO_2} K_{CH_4} P_{CO_2} P_{CH_4}}{\left(1 + K_{CO_2} P_{CO_2} + K_{CH_4} P_{CH_4}\right)^2} \quad (7)$$

$$k_{CO_2} = 1.17 \times 10^7 \exp\left(-\frac{83,498}{RT}\right), \quad (\mathrm{mol \cdot m^{-3} \cdot s^{-1}}) \quad (8)$$

$$K_{CO_2} = 3.11 \times 10^{-3} \exp\left(\frac{49,220}{RT}\right), \quad \mathrm{atm^{-1}} \quad (9)$$

$$K_{CH_4} = 0.653 \exp\left(\frac{16,054}{RT}\right), \quad \mathrm{atm^{-1}} \quad (10)$$

where T is temperature (K). R is the ideal gas constant (8.3145 J mol^{-1} K^{-1}). K_{CO_2} and K_{CH_4} are the adsorption equilibrium constants for CO_2 and CH_4, respectively. k_{CO_2} is the rate constant of MCDR. The reaction rates for MSR (R_{MSR}, mol m^{-3} s^{-1}) and WGSR (R_{WGSR}, mol m^{-3} s^{-1}) can be determined with the formula proposed by Haberman and Young [14],

$$R_{MSR} = k_{rf}\left(P_{CH_4} P_{H_2O} - \frac{P_{CO}\left(P_{H_2}\right)^3}{K_{pr}}\right) \quad (11)$$

$$k_{rf} = 2395 \exp\left(\frac{-231266}{RT}\right) \quad (12)$$

$$R_{WGSR} = k_{sf}\left(p_{H_2O} p_{CO} - \frac{p_{H_2} p_{CO_2}}{K_{ps}}\right) \quad (13)$$

$$k_{sf} = 0.0171 \exp\left(\frac{-103191}{RT}\right) \quad (\mathrm{mol \cdot m^{-3} \cdot Pa^{-2} \cdot s^{-1}}) \quad (14)$$

$$K_{ps} = \exp\left(-0.2935Z^3 + 0.6351Z^2 + 4.1788Z + 0.3169\right) \quad (15)$$

$$Z = \frac{1000}{T(K)} - 1 \quad (16)$$

$$K_{pr} = 1.0267 \times 10^{10} \times \exp\left(-0.2513Z^4 + 0.3665Z^3 + 0.5810Z^2 - 27.134Z + 3.277\right) \quad (17)$$

Table 1 – Parameters used in simulation.

Parameter	Value
Operating temperature, T (K)	1073
Operating pressure, P (bar)	1.0
Electrode porosity, ε	0.4
Electrode tortuosity, ξ	3.0
Average pore radius, r_p (μm)	0.5
Anode-supported electrolyte:	
Anode thickness d_a (μm)	500
Electrolyte thickness, L (μm)	100
Cathode thickness, d_c (μm)	100
Height of gas flow channel (mm)	1.0
Length of the planar SOFC (mm)	20
Thickness of interconnector (mm)	0.5
Inlet velocity at anode: U_o (m s^{-1})	1.0
Cathode inlet gas molar ratio: O_2/N_2	0.21/0.79
Anode inlet gas molar ratio: CH_4/CO_2 (landfill gas)	0.5/0.5
SOFC operating potential (V)	0.5
Thermal conductivity of SOFC component (W m^{-1} K^{-1})	
Anode	11.0
Electrolyte	2.7
Cathode	6.0
Interconnect	1.1

where K_{pr} and K_{ps} are the equilibrium constant for MSR and WGSR, respectively. k_{rf} and k_{sf} are the reaction constants for MSR and WGSR, respectively.

The reaction heats for MSR (H_{MSR}, J mol^{-1}), MCDR (H_{MCDR}, J mol^{-1}), and WGSR (H_{WGSR}, J mol^{-1}) can be determined as [15,16],

$$H_{MSR} = -(206205.5 + 19.5175T) \quad (18)$$

$$H_{MCDR} = -(253550.0 + 5.41667T) \quad (19)$$

$$H_{WGSR} = 45063 - 10.28T \quad (20)$$

The negative sign in H_{MSR} and H_{MCDR} indicates that both reactions are endothermic and consume heat.

2.2. Electrochemical reactions

The H_2 and CO molecules produced from the chemical reactions diffuse to the triple-phase boundary (TPB) at the anode-electrolyte interface where electrochemical reactions

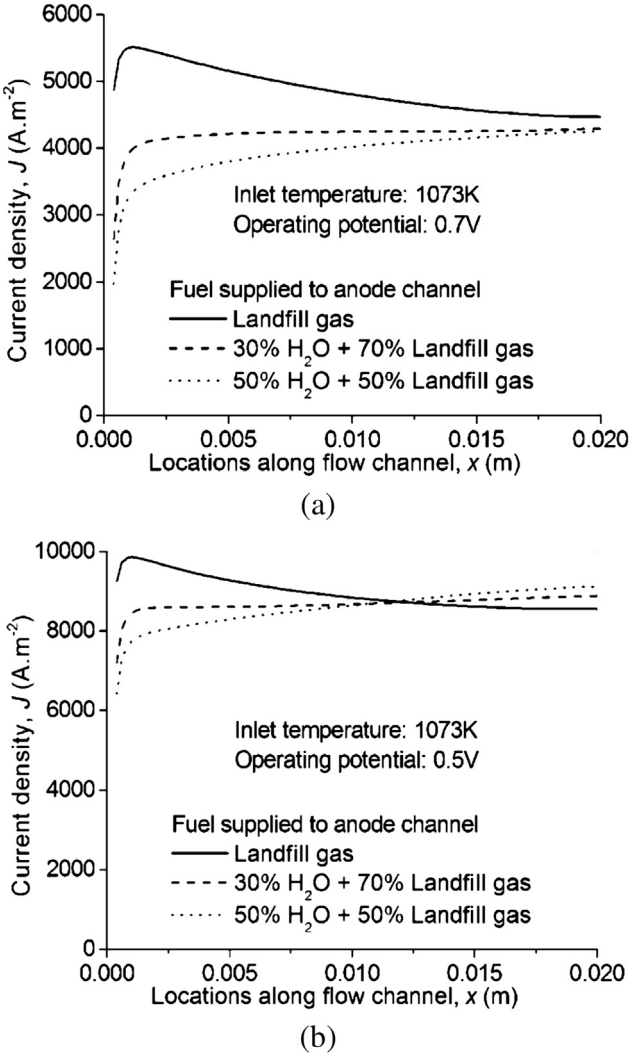

Fig. 2 – Effect of H_2O addition at 1073 K – comparison of current density distribution at operating potential of: (a) 0.7 V and (b) 0.5 V.

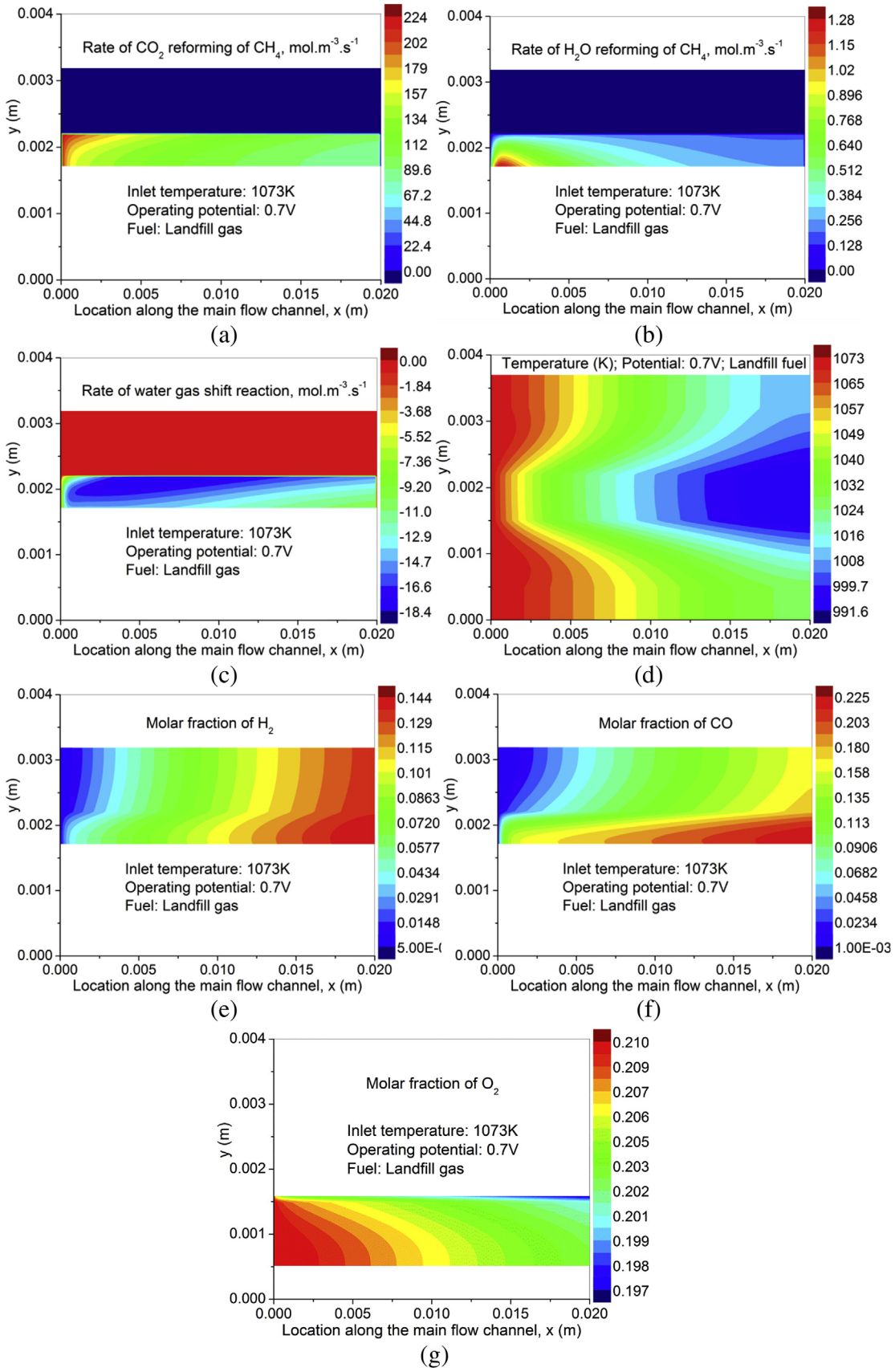

Fig. 3 – SOFC running on landfill gas at 1073 K and 0.7 V – (a) reaction rate of MCDR; (b) reaction rate of MSR; (c) reaction rate of WGSR; (d) temperature; (e) molar fraction of H_2; (f) molar fraction of CO; and (g) molar fraction of O_2.

occur. The rate of electrochemical reaction can be represented by the current density. Thus, an electrochemical model is developed to determine the local current density at given operating potentials (V). At zero current density (thus zero electrochemical reaction), the corresponding cell potential is the open-circuit voltage (OCV). Once current is drawn from the cell, the cell potential is decreased due to various overpotential losses. Thus the operating potential (V) can be evaluated as [17,18],

$$V = E\text{-}\eta_{act,a}\text{-}\eta_{act,c}\text{-}\eta_{ohmic} \quad (21)$$

here E is the OCV. $\eta_{act,a}$, $\eta_{act,c}$, and η_{ohmic} are the activation (anode and cathode) and ohmic overpotentials respectively.

Since both H_2 and CO are involved in electrochemical reactions, the Nernst potentials for H_2 fuel and CO fuel can be determined as [16],

$$E_{H_2} = 1.253\text{-}0.00024516T + \frac{RT}{2F}\ln\left[\frac{P^I_{H_2}\left(P^I_{O_2}\right)^{0.5}}{P^I_{H_2O}}\right] \quad (22)$$

$$E_{CO} = 1.46713 - 0.0004527T + \frac{RT}{2F}\ln\left[\frac{P^I_{CO}\left(P^I_{O_2}\right)^{0.5}}{P^I_{CO_2}}\right] \quad (23)$$

F is the Faraday constant (96,485 C mol^{-1}). In Eqs (22) and (23), the gas partial pressures (P^I) at the TPB are used, thus the concentration overpotentials are actually included in the Nernst equation. The activation overpotential represents the voltage loss due to electrochemical reactions and can be

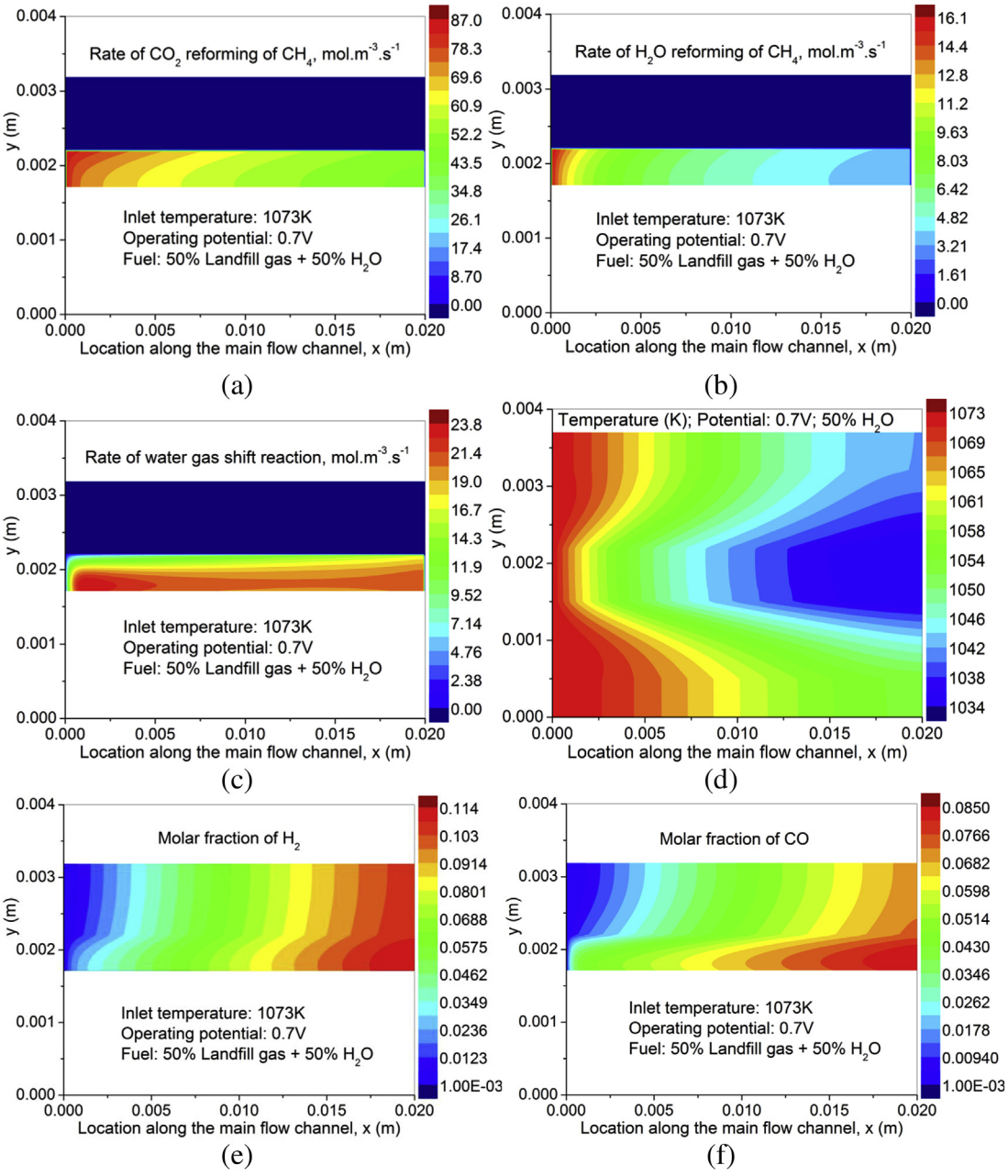

Fig. 4 – SOFC running on 50% H_2O + 50% landfill gas at 1073 K and 0.7 V – (a) reaction rate of MCDR; (b) reaction rate of MSR; (c) reaction rate of WGSR; (d) temperature; (e) molar fraction of H_2; and (f) molar fraction of CO.

approximately determined by $\eta_{act} = \frac{RTJ}{nFJ^0}$, where J is the current density (A m^{-2}), n is the number of electron involved in each electrochemical reaction and J^o is the exchange current density (A m^{-2}). The ohmic overpotential represents the voltage drop due to the transport of electrons and ions. As the ohmic loss in the electrodes is much lower than that in the electrolyte, only the ohmic loss due to oxide ion transport through the dense electrolyte is considered. According to the Ohm's law, the overpotential can be determined as $\eta_{ohmic} = JL\frac{1}{\sigma}$, where L and σ (Ω^{-1} m^{-1}) are the thickness and ionic conductivity of the electrolyte. For YSZ electrolyte, the ionic conductivity can be determined as $\sigma = 3.34 \times 10^4 \exp\left(-\frac{10300}{T}\right)$ [17]. The details of the electrochemical model can be found in Refs. [3,16].

2.3. Fluid flow, heat and mass transfer in SOFC

At typical gas velocity of 1 m s^{-1} in the channel and channel hydraulic diameter of about 1 mm, the Reynolds number in the channel is much smaller than 100, laminar flow is adopted in SOFC modeling. Thermal radiation is neglected in the present study and the temperatures of the gas and local thermal equilibrium assumption is adopted for the porous electrodes [19]. The governing equations for fluid flow, heat and mass transfer in SOFC are summarized below [20].

$$\frac{\partial(\rho U)}{\partial x} + \frac{\partial(\rho V)}{\partial y} = S_m \tag{24}$$

$$\frac{\partial(\rho UU)}{\partial x} + \frac{\partial(\rho VU)}{\partial y} = -\frac{\partial P}{\partial x} + \frac{\partial}{\partial x}\left(\mu\frac{\partial U}{\partial x}\right) + \frac{\partial}{\partial y}\left(\mu\frac{\partial U}{\partial y}\right) + S_x \tag{25}$$

$$\frac{\partial(\rho UV)}{\partial x} + \frac{\partial(\rho VV)}{\partial y} = -\frac{\partial P}{\partial y} + \frac{\partial}{\partial x}\left(\mu\frac{\partial V}{\partial x}\right) + \frac{\partial}{\partial y}\left(\mu\frac{\partial V}{\partial y}\right) + S_y \tag{26}$$

$$\frac{\partial\left(\rho c_{P,eff} UT\right)}{\partial x} + \frac{\partial\left(\rho c_{P,eff} VT\right)}{\partial y} = \frac{\partial}{\partial x}\left(k_{eff}\frac{\partial T}{\partial x}\right) + \frac{\partial}{\partial y}\left(k_{eff}\frac{\partial T}{\partial y}\right) + S_T \tag{27}$$

$$\frac{\partial(\rho UY_i)}{\partial x} + \frac{\partial(\rho VY_i)}{\partial y} = \frac{\partial}{\partial x}\left(\rho D_{i,m}^{eff}\frac{\partial Y_i}{\partial x}\right) + \frac{\partial}{\partial y}\left(\rho D_{i,m}^{eff}\frac{\partial Y_i}{\partial y}\right) + S_{sp} \tag{28}$$

where ρ and μ are the density and viscosity of the gas mixture and depends on the gas composition. U and V are the velocity components in x and y directions respectively. k_{eff} and $c_{p,eff}$ are the effective heat conductivity and heat capacity of the gas mixture (in the gas channel) and the mixture of the gas and solid particles (in the porous electrodes). Y_i is the mass fraction of gas species i. $D_{i,m}^{eff}$ is the effective diffusion coefficient of species i in the gas mixture. S is the source term. The details on the effective diffusion coefficient, effective heat conductivity, and heat capacity for momentum equations (Eqs. (25) and (26)), energy equation (Eq. (27)) and species equation (Eq.

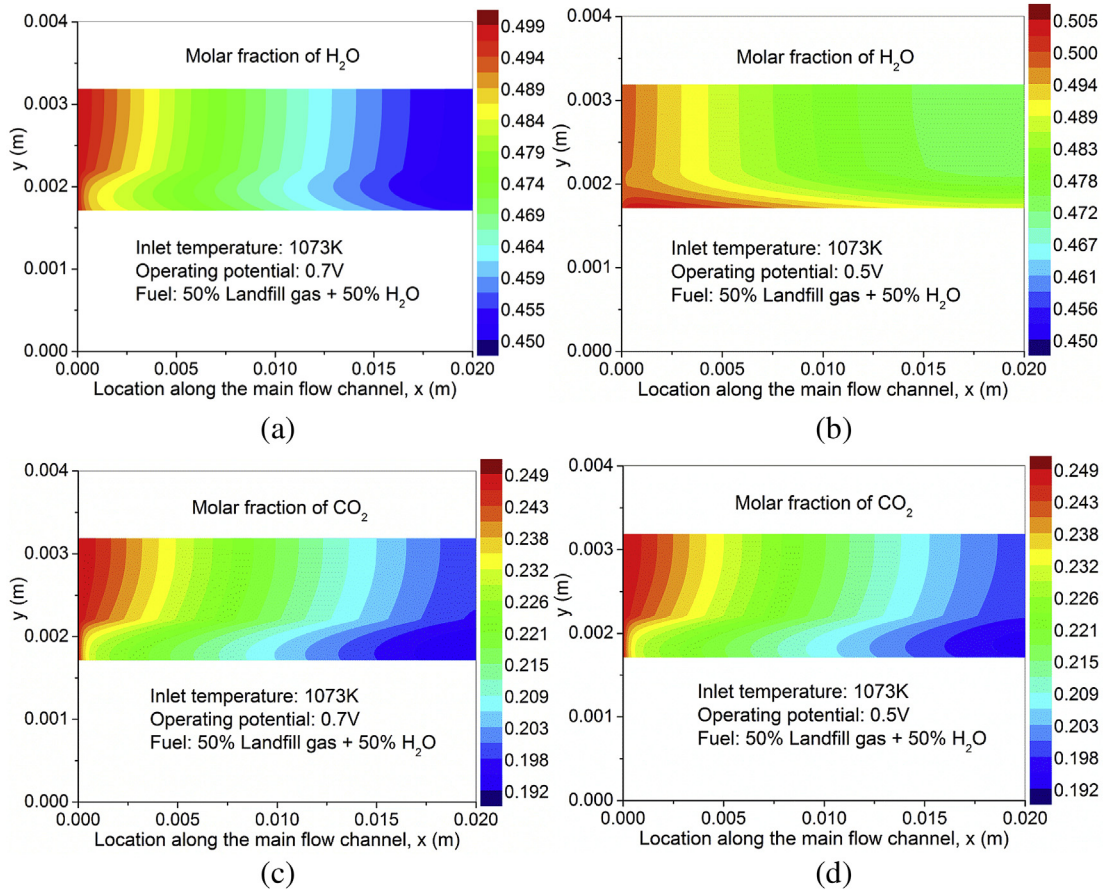

Fig. 5 – Gas composition in SOFC running on 50% H_2O + 50% landfill gas at 1073 K – (a) molar fraction of H_2O at operating potential of 0.7 V; (b) molar fraction of H_2O at operating potential of 0.5 V; (c) molar fraction of CO_2 at operating potential of 0.7 V; and (d) molar fraction of CO_2 at operating potential of 0.5 V.

(28)) can be found in the previous publication [3,16]. The source terms in Eq. (24)–(28) are very important parameters. The source term (S_m) in Eq. (24) represents the mass increase in the anode and mass reduction in the cathode, as oxygen ions are transported from the cathode to the anode. The Darcy's law is used as the source terms (S_x and S_y) in Eqs. (25) and (26) so that the momentum equations can be applicable to both the gas channels and the porous electrode layers. The source term (S_T) in Eq. (27) accounts for the heat consumption by MSR and MCDR reaction and heat generation by WGSR and electrochemical reactions. The source term (S_{sp}) in Eq. (28) represents the species generation or consumption due to the chemical (in the whole anode layer) and electrochemical (at the electrode-electrolyte interface) reactions. Details can be found in Refs. [3,16]. The detailed procedures are not repeated here to avoid duplication.

2.4. *Numerical methods*

The boundary conditions of the 2D model can be found in Ref. [21]. The finite volume method (FVM) is adopted for solving the model. The SIMPLEC algorithm is used to couple the velocity and pressure terms. The program starts from initialization. Initial values of parameters, such as temperature, pressure, velocity, gas composition etc, are assigned to the entire computational domain. The chemical reaction kinetics and the corresponding reaction heats are calculated. Then the local current density (electrochemical reaction rate) and corresponding heat are solved at given operating potentials. The results from chemical reaction module and electrochemical module are used to calculate the source terms of the fluid flow and heat/mass transfer module. After the flow field and temperature field are solved, convergence check is conducted. If the results are not converged, calculation will be repeated using the updated values (temperature, pressure, gas composition etc). The computation will continue till converged results are achieved. The in-house code is developed in FORTRAN and has been validated by comparing the simulation results with literature data. Details can be found in Ref. [21].

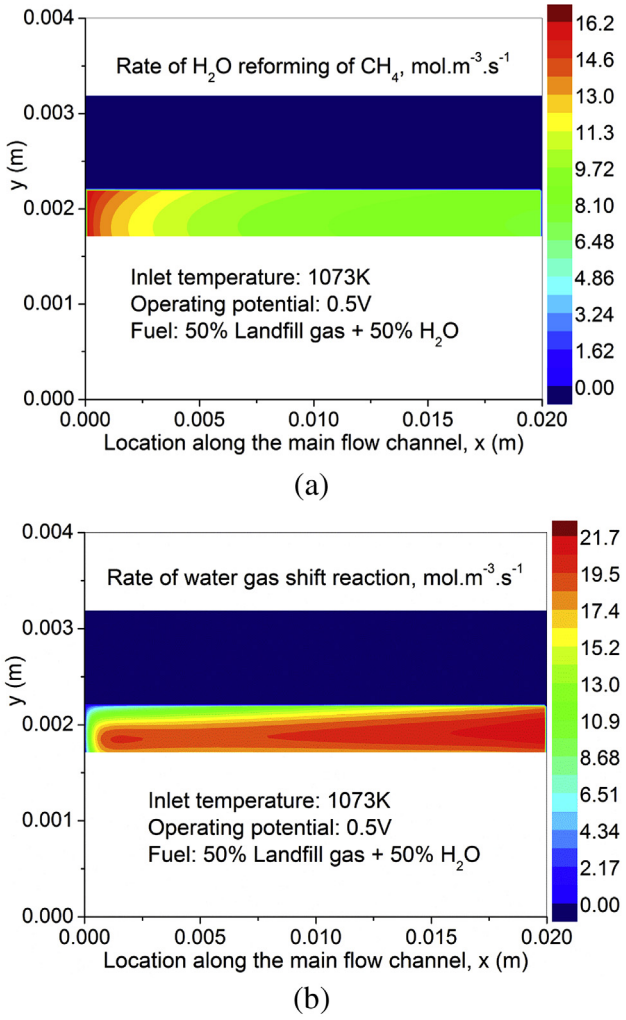

Fig. 6 – SOFC running on 50% H_2O and 50% landfill gas at 1073 K and 0.5 V – (a) MSR reaction rate; and (b) WGSR rate.

3. Results and discussion

In this section, simulations are performed to investigate the effects of various operating parameters particularly the H_2O

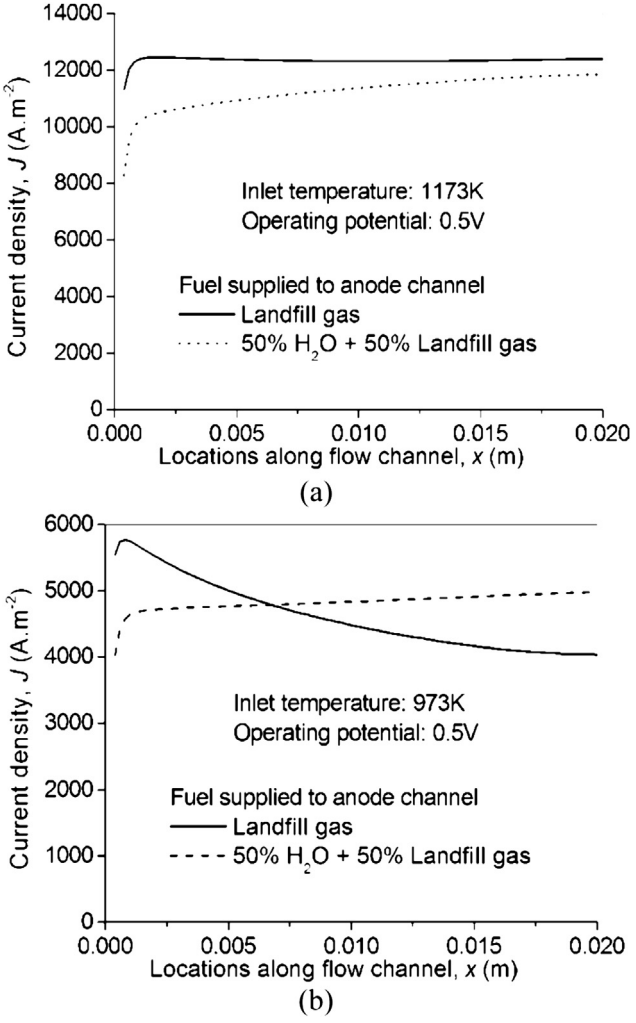

Fig. 7 – Current density of SOFC running on landfill gas and 50% H_2O + 50% landfill gas mixture at 0.5 V – (a) 1173 K and (b) 973 K.

addition on landfill gas fueled SOFC performance. The values of input parameters are summarized in Table 1. Simulations are performed at typical operating potentials of 0.7 V and 0.5 V and typical inlet temperature of 1073 K. To examine the H_2O addition effect, three cases are considered as fuel at the anode inlet: 100% landfill gas (50% CH_4 + 50% CO_2), 30% H_2O + 70% landfill gas, and 50% H_2O + 50% landfill gas.

3.1. *Base case – effect of H_2O addition*

The computed current density distribution of landfill gas fueled SOFC is shown in Fig. 2. As can be seen, the current density is the highest without H_2O addition (100% landfill gas) at an inlet temperature of 1073 K and operating potential of 0.7 V, especially near the inlet (Fig. 2a). In the downstream, the current density of landfill gas fueled SOFC is decreased while that of SOFC with H_2O addition is slightly increased (particularly with 50% H_2O addition). With a decrease in operating potential from 0.7 V to 0.5 V, it can be seen that the current density in the downstream of SOFC with H_2O addition surpasses that of SOFC running on 100% landfill gas (Fig. 2b).

To understand these phenomenon, the distributions of reaction rates, temperature and gas composition in landfill gas fueled SOFC are studied and shown in Fig. 3. As can be seen from Fig. 3a, the rate of MCDR is the highest (about 224 mol m^{-3} s^{-1}) at the SOFC inlet and decreases significantly

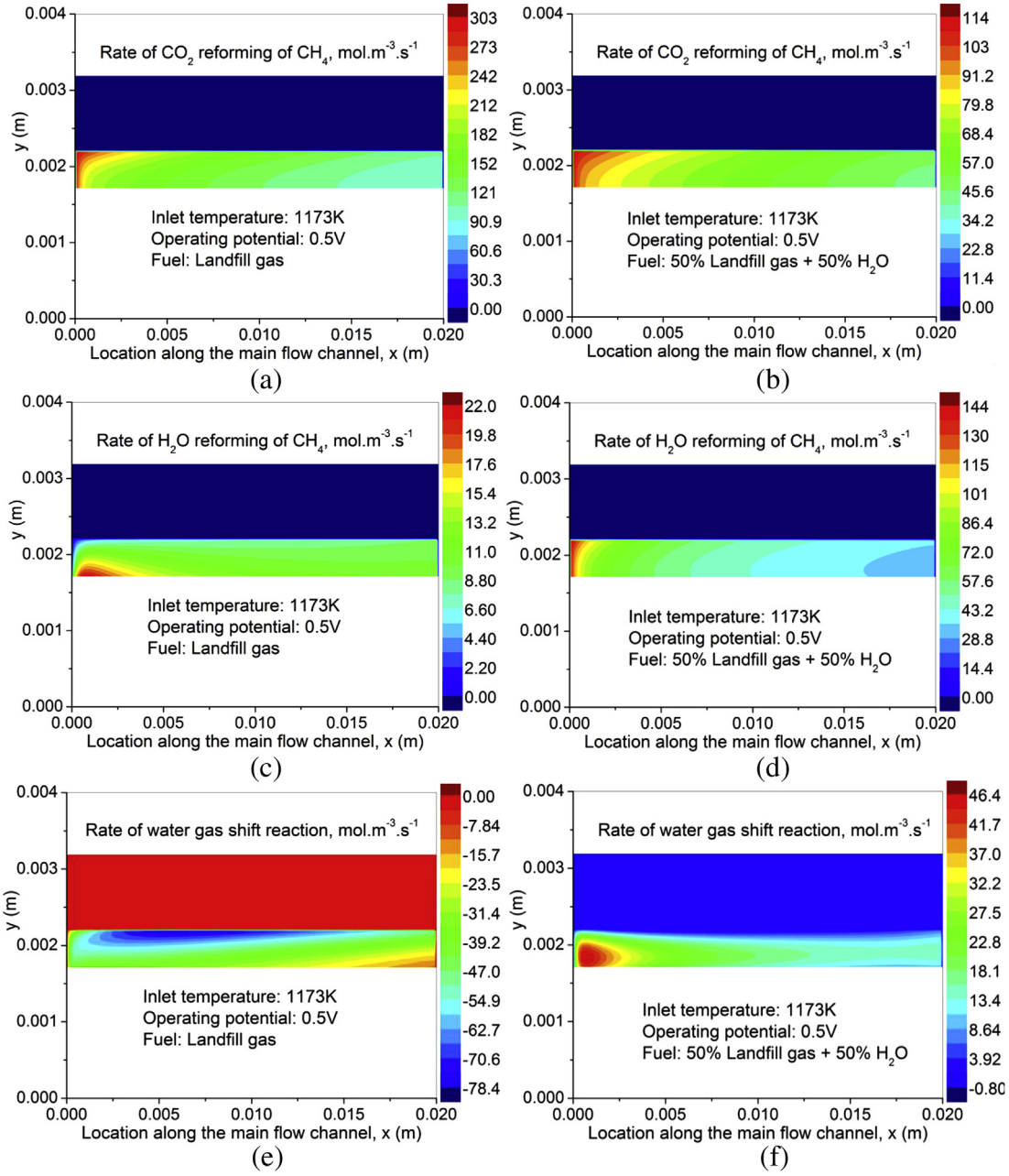

Fig. 8 – Comparison between SOFC running on landfill gas and on 50% landfill gas + 50% H_2O at 1173 K and 0.5 V – (a) MCDR rate with landfill gas; (b) MCDR rate with 50% landfill gas + 50% H_2O; (c) MSR rate with landfill gas; (d) MSR rate with 50% landfill gas + 50% H_2O; (e) WGSR rate with landfill gas; and (f) WGSR rate with 50% landfill gas + 50% H_2O.

along the flow channel. The calculated MCDR reaction rate is consistent with the experimental data from Refs. [13,22]. Prof. Yentekakis's group has tested SOFC with MCDR [23–25]. They reported higher rate of MCDR of about 416 mol m^{-3} s^{-1} with Ni-YSZ cermet electrode (prepared from wet-impregnation) at an operating temperature of 1073 K [23], which is higher than but still on the same order with the present computed data. Thus, although the kinetics on Ru/γ-Al_2O_3/Ni–Cr–Al is adopted in the present study, it still approximates the kinetics of MCDR in SOFC. The model can be improved once more reliable information about MCDR in SOFC is available. The calculated rate of MSR is very low (1.28 mol m^{-3} s^{-1} the highest) as 100% landfill gas is used at the anode and thus the H_2O concentration is low (Fig. 3b). The WGSR is found negative in SOFC (Fig. 3c). This is due to the low H_2O concentration in the cell which favors backward WGSR. Both MSR and MCDR are endothermic and consume heat. The WGSR is exothermic but the negative WGSR becomes endothermic. On the other hand, the electrochemical reactions and the overpotential losses generate heat. The large temperature drop in the cell from 1073 K at the inlet to about 991 K at the outlet reveals that the heat absorption by chemical reactions is significantly higher than heat generation by electrochemical reactions and overpotential losses (Fig. 3d). Due to the high rate of MCDR, the molar fractions of both H_2 and CO are found to increase along the flow channel (Figs. 3e and f). Moreover, relatively large concentration difference between the fuel channel and the porous anode is observed for CO fuel (Fig. 3f). This is because

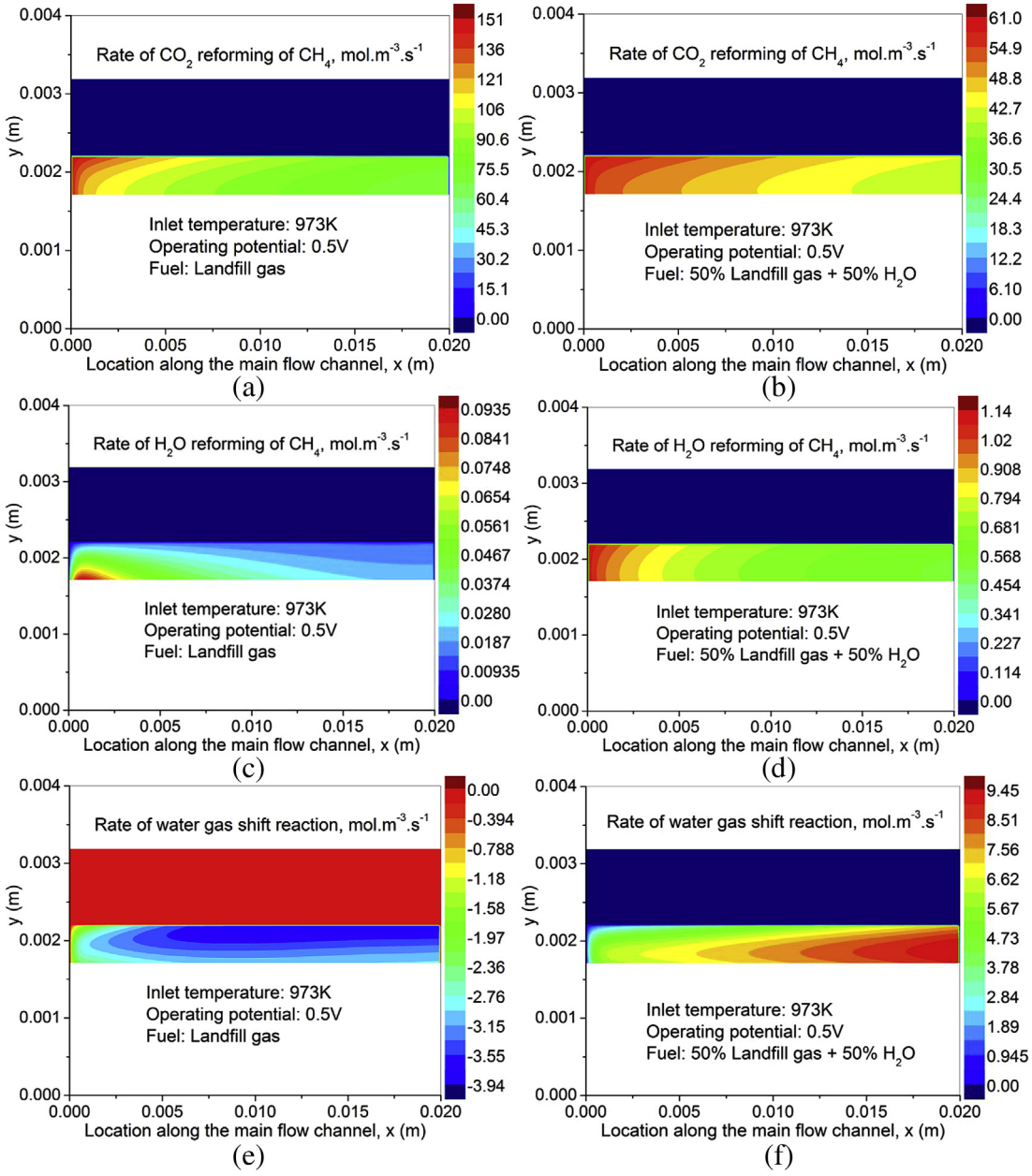

Fig. 9 – Comparison between SOFC running on landfill gas and on 50% landfill gas + 50% H_2O at 973 K and 0.5 V – (a) MCDR rate with landfill gas; (b) MCDR rate with 50% landfill gas + 50% H_2O; (c) MSR rate with landfill gas; (d) MSR rate with 50% landfill gas + 50% H_2O; (e) WGSR rate with landfill gas; and (f) WGSR rate with 50% landfill gas + 50% H_2O.

the effective diffusion coefficient for CO molecules is smaller than that for H_2 molecules [3,16], causing slower CO diffusion and thus larger concentration variation in the porous layer. Similarly, the diffusion of O_2 in the cathode is also slow due to its large molecular weight. As shown Fig. 3g, the concentration difference between the air channel and the porous cathode is obvious but not very high since relatively thin cathode (0.1 mm) is used in the simulation.

For comparison, the distributions of reaction rates, temperature and gas composition in the SOFC running on 50% landfill gas + 50% H_2O are shown in Fig. 4. Compared with the 100% landfill gas case (Figs. 3a and b), the computed MCDR reaction rate is considerably lower (87 mol m^{-3} s^{-1} the highest) but the MSR reaction rate is increased (peak at about 16.1 mol m^{-3} s^{-1}) with 50% H_2O addition (Figs. 4a and b), as H_2O addition favors MSR but dilute the concentrations of both CH_4 and CO_2. The calculated MSR reaction rate is consistent with the data in Refs. [14,26]. In Haberman and Young's simulation [14], it is found that MSR reaction rate is highly temperature-dependent – negligibly small at $T < 1100$ K and increased significantly at $T > 1173$ K. The good agreement between the presently calculated MSR reaction rate and the literature data again validates the present model. In addition, positive WGSR is found in SOFC (Fig. 4c), which differs from the 100% landfill gas case (Fig. 3c). Compared with the 100% landfill gas case (Fig. 3d), the temperature reduction in SOFC is much smaller with 50% H_2O addition (Fig. 4d). Although the current density is lower and the MSR reaction rate is higher for the latter case, the greatly reduced MCDR reaction rate consumes less heat and positive WGSR generates heat. As a result, the temperature is decreased by about 39 K from 1073 K at the inlet and 1034 K at the outlet. However, the significant reduction in MCDR reaction rate also decreases H_2 and CO production (Fig. 4e and f), although MSR reaction rate is increased. Comparing the two cases, it can be seen that the H_2 molar fraction at the SOFC outlet is decreased from about 0.14 (Fig. 3e) to about 0.11 (Fig. 4e). For CO, larger reduction is observed (Figs. 3f and 4f), as positive WGSR consumes CO with 50% H_2O addition.

As the operating potential is decreased from 0.7 V to 0.5 V, the current density is greatly increased (Fig. 2), which tends to produce more H_2O and CO_2 from electrochemical reactions. It can be seen from Fig. 5a–d, the molar fraction of H_2O and CO_2 in the downstream of the SOFC is increased when the potential is decreased to 0.5 V. The effect of operating potential on CO_2 is less significant than on H_2O, due to lower electrochemical oxidation rate of CO than that of H_2 [11]. As a result, the reaction rates of MSR and WGSR in the SOFC downstream are found improved at 0.5 V, compared with 0.7 V (Fig. 6a and b).

From the above analyses, it can be seen that at a typical inlet temperature of 1073 K, H_2O addition to the fuel stream lowers the SOFC performance near the inlet as it dilute the concentration of landfill gas. However, addition of H_2O tends

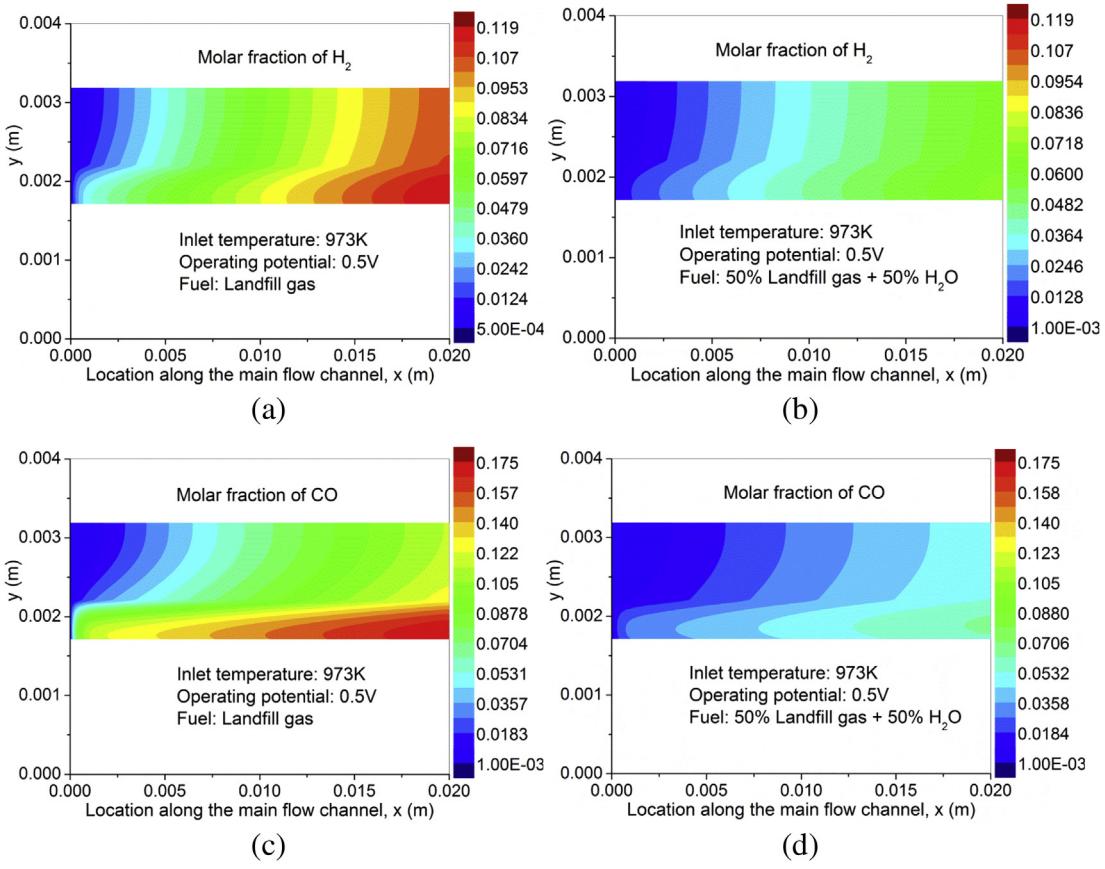

Fig. 10 – Comparison between SOFC running on landfill gas and on 50% landfill gas + 50% H_2O at 973 K and 0.5 V – (a) molar fraction of H_2 with landfill gas; (b) molar fraction of H_2 with 50% landfill gas + 50% H_2O; (c) molar fraction of CO with landfill gas; and (d) molar fraction of CO with 50% landfill gas + 50% H_2O.

to increase the SOFC performance in the downstream and at a reduced operating potential.

3.2. *Effect of inlet temperature*

In this section, simulations are performed at inlet temperatures of 973 K and 1173 K. The computed current density from SOFC running on 100% landfill gas and 50% landfill gas + 50% H_2O are shown in Fig. 7. As can be seen from Fig. 7a, at a higher inlet temperature (1173 K), the current density in SOFC running on 100% landfill gas is higher than that on 50% landfill gas + 50% H_2O. For comparison, at a lower inlet temperature (973 K), addition of H_2O is beneficial in increasing the current density, particularly in the downstream (Fig. 7b).

To elucidate the temperature effect, the reaction rates in SOFC are calculated at different inlet temperatures of 973 K and 1173 K and shown in Figs. 8 and 9. As can be seen, addition of H_2O significantly decreases the MCDR reaction rate (Figs. 8a and b) but increases the MSR reaction rates (Fig. 8c and d). Moreover, the WGSR rate is negative without H_2O addition and positive with addition of 50% H_2O in the fuel stream (Fig. 8e and f). The lower MCDR reaction with H_2O addition explains why the current density is lower than that without H_2O addition (Fig. 7a) while the higher MSR reaction and positive WGSR rates with H_2O addition tend to reduce the difference between these two cases.

At an inlet temperature of 973 K, the reaction rate distributions are similar to those at 1173 K (Fig. 9a–f), i.e. addition of H_2O decreases MCDR reaction rate. However, the variation in MCDR reaction rate along the gas channel is found to be smaller with H_2O addition (Fig. 9b). MSR reaction rates are very low in both cases due to the low temperature (Fig. 9c and d). High WGSR rate is found in the downstream of SOFC with H_2O addition (Fig. 9f). Due to the large reduction in MCDR reaction rate, the molar fractions of H_2 and CO are both found lower with H_2O addition (Fig. 10a–d). On the other hand, the reduced MCDR reaction rate absorbs less heat and the positive WGSR generates heat. As a result, the temperature in the downstream of SOFC with H_2O addition is found much higher than that without H_2O addition (Fig. 11a and b), which explains why the downstream current density is higher with H_2O addition (Fig. 7b).

3.3. *SOFC with longer channel*

From the above analyses, it can be seen that H_2O addition tends to enhance the SOFC performance in the downstream, particularly at reduced temperature and lower operating potential. In this section, additional simulations are performed for SOFC with longer gas channels (40 mm). The computed current density in SOFC is shown in Fig. 12. The SOFC performance is found to increase with increasing H_2O addition (up to 50% in the present simulation). Thus, H_2O addition is needed for SOFC with long channel at reduced temperature.

3.4. *SOFC with various flow rates*

In this section, the effects of flow rates on the cell performance are investigated by varying the gas velocity at the

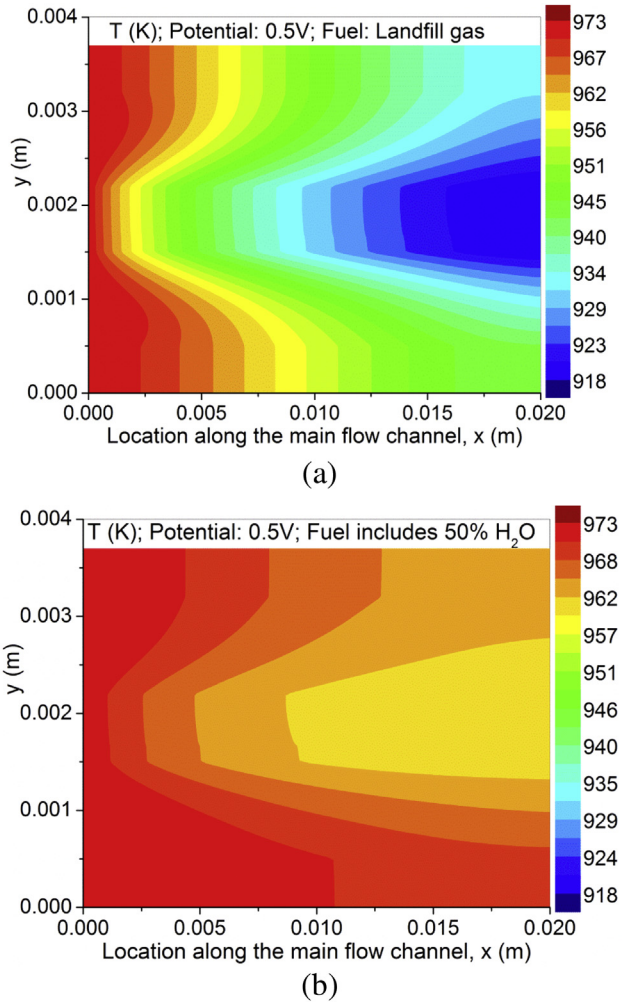

Fig. 11 – Temperature in SOFC at operating potential of 0.5 V – (a) with landfill gas; and (b) with 50% landfill gas + 50% H_2O.

anode inlet from 1 m s^{-1} to 0.5 m s^{-1} and 3.0 m s^{-1}. As can be seen from Fig. 13a, the beneficial effect of steam addition in the downstream is more significant at a lower gas velocity (flow rate), as decreasing the flow rate is equivalent to an increase in the cell length. For comparison, the effect of steam addition in the downstream is decreased (Fig. 13b), since increasing flow rate is equivalent to a decrease in the cell length.

3.5. *Landfill gas composition effect*

As the landfill gas composition could be very different in different countries, it is useful to investigate how the H_2O effect at different CO_2/CH_4 ratio. In the previous study, when the ratio of CO_2 to CH_4 is smaller than 50/50, O_2 is used to reform CH_4 to CO and H_2 [8]. Thus, if CO_2 is insufficient to reform CH_4, O_2 or H2O is needed. In this section, the molar ratio of CO_2 to CH_4 is changed to 70/30 to investigate the H_2O effect. The computed current density is shown in Fig. 14. As can be seen, the addition of 30% H_2O into the fuel stream also tends to

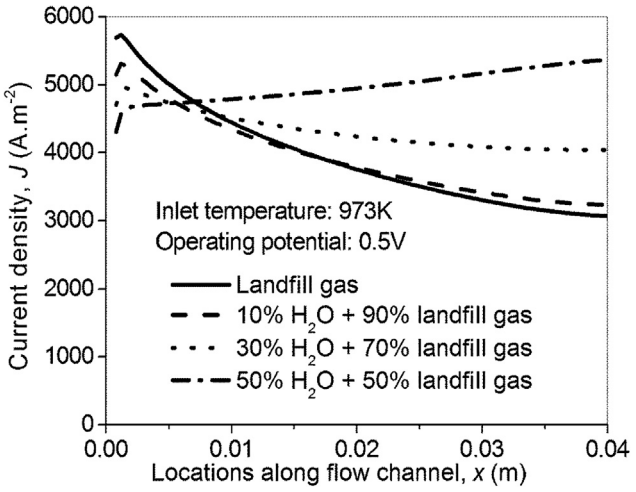

Fig. 12 – Comparison of current density at inlet temperature of 973 K, operating potential of 0.5 V, and cell length of 40 mm.

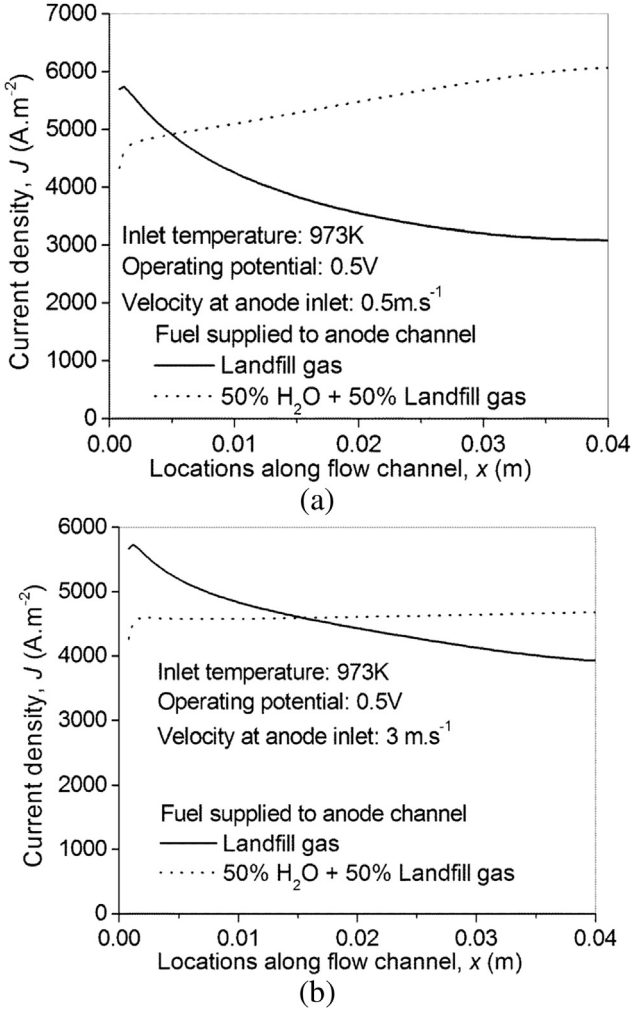

Fig. 13 – Current density of SOFC running on landfill gas and 50% H_2O + 50% landfill gas mixture at 973 K and 0.5 V – (a) inlet gas velocity of 0.5 m s^{-1} and (b) inlet gas velocity of 3 m s^{-1}.

increase the cell performance in the downstream. Without H_2O addition, the WGSR is strongly negative (Fig. 15a), which converts H_2 and CO_2 into CO and H_2O. For comparison, with 30% H_2O in the fuel stream, the WGSR becomes positive (although still slightly negative in some region) (Fig. 15b), which in turn converts CO and H_2O to H_2 and CO_2. As electrochemical oxidation of H_2 is faster than that of CO, positive WGSR is beneficial for SOFC performance. In addition, WGSR is exothermic thus negative reaction rates tend to decrease the cell temperature. Thus, the temperature of SOFC running on landfill gas is found to decrease significantly along the gas channel (Fig. 15c), lower than the case with 30% H_2O (Fig. 15d). The combined effects results in enhanced performance in the downstream when H_2O is added.

4. Conclusion

A 2D numerical model is developed to simulate the physical and chemical processes in SOFC running on landfill gas. Parametric simulations are performed to exam whether addition of H_2O into the fuel stream is beneficial for SOFC or not. It is found that due to the reforming reaction of CH_4 by CO_2, addition of H_2O into the fuel stream in general diluate the fuel concentration and thus decreases the cell performance of SOFC with short length (2 cm). However, at a low operating potential or a lower temperature, or a longer SOFC, addition of H_2O tends to increase the cell performance, especially in the downstream of SOFC. This is because H_2O facilitates positive WGSR, which: (1) converts H_2O and CO to CO_2 and H_2 (easier for electrochemical oxidation than CO) and (2) tends to increase the cell temperature. These results indicate that for a real SOFC with longer gas channel, addition of a certain amount of H_2O into the landfill gas is necessary at certain operating conditions. Considering that steam addition consumes more thermal energy for heating up water to the inlet temperature of the cell, there will be an optimal steam concentration which can yields the highest energy efficiency

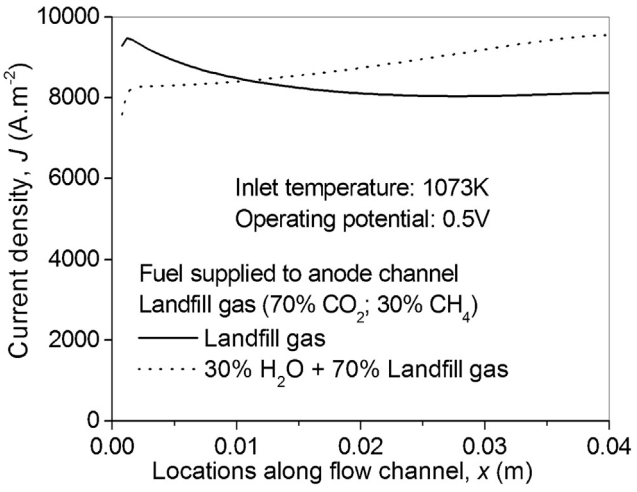

Fig. 14 – Current density of SOFC running on landfill gas (70% CO_2 + 30% CH_4) and 70% landfill gas + 30% H_2O at 1073 K and 0.5 V.

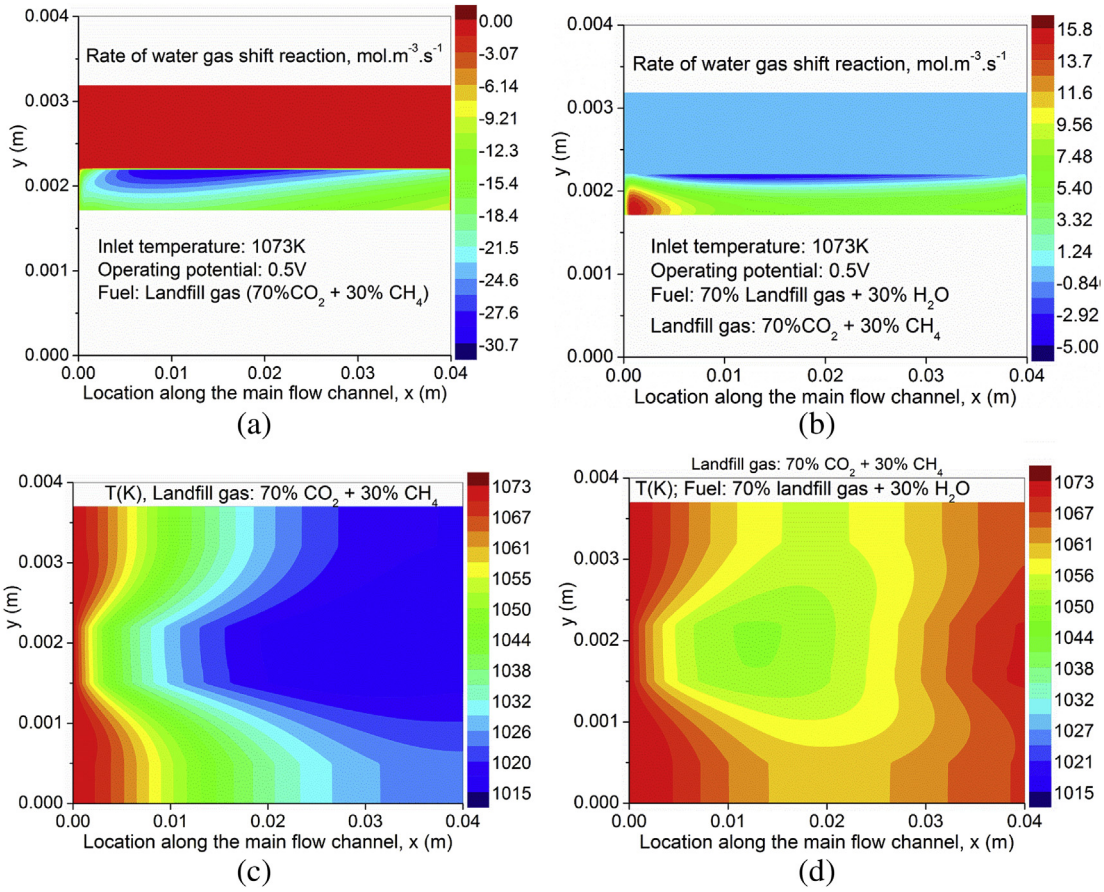

Fig. 15 – SOFC running on landfill gas (70% CO_2 + 30% CH_4) and 70% landfill gas + 30% H_2O at 1073 K and 0.5 V – (a) WGSR rate with landfill gas; (b) WGSR rate with 70% landfill gas + 30% H_2O; (c) temperature with landfill gas; and (d) temperature with 70% landfill gas + 30% H_2O.

of the SOFC system. As part of an ongoing project on landfill gas fueled SOFC, a thermodynamic analysis of the SOFC-based cogeneration system will be conducted in a subsequent study.

Acknowledgment

This research is supported by a fund from Department of Building and Real Estate, The Hong Kong Polytechnic University (Project No: **4-ZZC3**).

REFERENCES

[1] http://re.emsd.gov.hk/english/energy/landfill/land_tech.html. [accessed 07.10.13.
[2] Singhal SC, Kendall K. High temperature solid oxide fuel cells – fundamentals, design and applications. New York: Elsevier; 2003.
[3] Ni M. Modeling of SOFC running on partially pre-reformed gas mixture. Int J Hydrogen Energy 2012;37:1731–45.
[4] Ma QL, Peng RR, Lin YJ, Gao JF, Meng GY. A high-performance ammonia-fueled solid oxide fuel cell. J Power Sources 2006;161:95–8.
[5] Ni M, Leung DYC, Leung MKH. Mathematical modeling of ammonia-fed solid oxide fuel cells with different electrolytes. Int J Hydrogen Energy 2008;33:5765–72.
[6] Ni M, Leung DYC, Leung MKH, Sumathy K. An overview of hydrogen production from biomass. Fuel Process Technol 2006;87:461–72.
[7] Wang W, Su C, Ran R, Shao ZP. A new Gd-promoted nickel catalyst for methane conversion to syngas and as an anode functional layer in a solid oxide fuel cell. J Power Sources 2011;196:3855–62.
[8] Staniforth J, Kendall K. Cannock landfill gas powering a small tubular solid oxide fuel cell – a case study. J Power Sources 2000;86:401–3.
[9] Wartsila. SOFC using landfill gas passes first phase field trial. Fuel Cells Bull 2010;3:5.
[10] Ni M. Modeling and parametric simulations of solid oxide fuel cells with methane carbon dioxide reforming. Energy Convers Manag 2013;70:116–29.
[11] Matsuzaki Y, Yasuda I. Electrochemical oxidation of H_2 and CO in a H_2–H_2O–CO–CO_2 system at the interface of a Ni-YSZ cermet electrode and YSZ electrolyte. J Electrochem Soc 2000;147:1630–5.
[12] Janardhanan VM, Deutschmann O. Numerical study of mass and heat transport in solid-oxide fuel cells running on humidified methane. Chem Eng Sci 2007;62:5473–86.
[13] Gokon N, Osawa Y, Nakazawa D, Kodama T. Kinetics of CO_2 reforming of methane by catalytically activated metallic foam absorber for solar receiver-reactors. Int J Hydrogen Energy 2009;34:1787–800.

[14] Haberman BA, Young JB. Three-dimensional simulation of chemically reacting gas flows in the porous support structure of an integrated-planar solid oxide fuel cell. Int J Heat Mass Trans 2004;47:3617–29.
[15] Chase MW. NIST-JANAF thermochemical tables. 4th ed. American Chemical Society, American Institute of Physics for the National Institute of Standards and Technology; 1998.
[16] Ni M. 2D thermal modeling of a solid oxide electrolyzer cell (SOEC) for syngas production by H_2O/CO_2 co-electrolysis. Int J Hydrogen Energy 2012;37:6389–99.
[17] Ni M, Leung MKH, Leung DYC. Parametric study of solid oxide fuel cell performance. Energy Convers Manag 2007;48:1525–35.
[18] Ni M. Electrolytic effect in solid oxide fuel cells running on steam/methane mixture. J Power Sources 2011;196:2027–36.
[19] Zheng KQ, Sun Q, Ni M. On the local thermal non-equilibrium in SOFCs considering internal reforming and ammonia thermal cracking reaction. Energy Technol 2013;1:35–41.
[20] Wang CY. Fundamental models for fuel cell engineering. Chem Rev 2004;104:4727–65.
[21] Ni M. 2D thermal-fluid modeling and parametric analysis of a planar solid oxide fuel cell. Energy Convers Manag 2010;51:714–21.
[22] Soloviev SO, Kapran AY, Orlyk SN, Gubareni EV. Carbon dioxide reforming of methane on monolithic Ni/Al_2O_3-based catalysts. J Nat Gas Chem 2011;20:184–90.
[23] Goula G, Kiousis V, Nalbandian L, Yentekakis IV. Catalytic and electrocatalytic behavior of Ni-based cermet anodes under internal dry reforming of CH4 + CO2 mixtures in SOFCs. Solid State Ionics 2006;177:2119–23.
[24] Yentekakis IV. Open- and closed-circuit study of an intermediate temperature SOFC directly fueled with simulated biogas mixtures. J Power Sources 2006;160:422–5.
[25] Papadam T, Goula G, Yentekakis IV. Long-term operation stability tests of intermediate and high temperature Ni-based anodes' SOFCs directly fueled with simulated biogas mixtures. Int J Hydrogen Energy 2012;37:16680–5.
[26] Lehnert W, Meusinger J, Thorn F. Modeling of gas transport phenomena in SOFC anodes. J Power Sources 2000;87:57–63.